12th International Conference on Fracture Mechanics of Concrete and Concrete Structures
FraMCoS-12
B.L.A. Pichler, Ch. Hellmich, P. Preinstorfer (Eds)

https://doi.org/10.21012/FC12.1238
MS05-3:3

INFLUENCE OF THE COMPRESSIVE FRACTURE ENERGY ON THE PREDICTED BREAKOUT FAILURE OF FASTENERS

JOHANNES HOLDER[*], HITESH LAKHANI[*] AND JAN HOFMANN[*]

[*] University of Stuttgart, Institute of Construction Materials (IWB)
Pfaffenwaldring 4, 70569 Stuttgart, Germany
e-mail: johannes.holder@iwb.uni-stuttgart.de, www.iwb.uni-stuttgart.de

Key words: Fracture Energy, Numerical Analysis, Fasteners in Concrete, Concrete Cone Failure

Abstract: Concrete Cone (CC) failure of fasteners remains a challenging engineering problem in numerical simulation due to the mixed-mode fracture. For this reason, design of fasteners still heavily depends on empirical design rules from standards which come with limitations in applicability. One less researched influencing factor in numerical simulations of CC-failure is the compressive fracture energy of concrete. In this paper, a numerical study is carried out in the commercial Finite-Element software ANSYS® Mechanical using Drucker-Prager model with Rankine's criterion i.e., the yield surface under compression is defined using Drucker-Prager criterion and the Rankine criterion bounds the tensile stresses for concrete. The influence of fracture energy under compression on the ultimate load and load-displacement behavior of fasteners under CC-failure as well the mesh-sensitivity is studied for two embedment depths. Strong influence of the compressive fracture energy on the ultimate load, load-displacement behavior and fracture pattern in the simulations could be identified.

1 INTRODUCTION

The use of numerical simulations in civil engineering has seen a massive rise in the last decades [1,2]. However, some aspects like the numerical simulation of fasteners in concrete are still a challenging task [3]. For fasteners in concrete, a variety of failure modes has to be considered. These failure modes can be caused by failure of the fastener, concrete failure or failure of the connection between fastener and concrete. The predominant failure mode for anchors loaded in tension is the Concrete Cone (CC) failure which involves complex fracture processes. In this case, the capacity of the fastener not only depends on the strength of the concrete but also on the fracture properties. The breakout of the concrete cone is a complex mixed-mode fracture. As a consequence, the design of fastening in concrete still heavily depends on empiric formulas in building standards, which are limited to simple fastening configurations and simple geometries. This has led to a steadily growing demand of advanced numerical models for designing in fastening technology.

One important aspect for the correct simulation of the fracture process in concrete is mesh-independency of results. This is usually achieved by implementation of fracture-energy based regularization in numerical modeling [4–6]. However, in contrast to the well-known concept of tensile fracture energy, the concept of compressive fracture energy is more limited. This limitation is mainly due to the significant influence of the specimen size and boundary conditions on the softening in stress-strain relationship under compression. Furthermore, the influence of tensile fracture energy and its regularization to achieve mesh independent results is well known and documented but the

choice of fracture energy under compression or the softening branch of the stress-strain curve under compression in numerical models is mostly based on assumptions and seldom discussed.

While many influencing factors like Young's Modulus and tensile fracture energy have been well researched for their influence on the CC-capacity of fasteners (e.g. [7,8]) there are –to the authors knowledge- no studies on the influence of compressive fracture energy on the CC-capacity of fasteners in concrete.

For this reason, a numerical study using the commercial Finite Element (FE) software ANSYS® Mechanical 2023 R2 [9] is carried out to investigate: a) the influence of the assumed compression fracture energy in the numerical model, on the predicted CC-capacity; b) if the experimentally measured compressive energy is a suitable input to the material model or this parameter should be numerically calibrated. For the numerical investigation presented and discussed in this paper a cast-in headed stud in concrete without any influence of the edges is simulated with two embedment depths. The concrete is modelled with Drucker-Prager model with Rankine's criterion i.e., the yield surface under compression is defined using Drucker-Prager criterion and the Rankine criterion bounds the tensile stresses for concrete. For this model, two different definitions of strain softening, viz., based on Eurocode 2 EN 1992-1-1 [10] and compression fracture energy-based definition, are used with different input parameters in terms of the ratio between compression and tension fracture energy (G_{fc}/G_{ft}) which result in a variety of compressive fracture energies. Furthermore, the mesh size sensitivity of the approach is checked.

2 MODEL PROPERTIES

2.1 Geometry, materials and constraints

For the numerical study, headed studs with an embedment depth of $h_{ef} = 50\,mm$ and $h_{ef} = 70\,mm$ are modelled using the commercial Finite Element (FE) software ANSYS® Mechanical 2023 R2 [9]. The mean compressive strength of concrete for a standard cylinder is taken as $f_{cm} = 24.73\ N/mm^2$. Since, the aim of the study is to investigate the CC-failure, the steel (for headed stud) is assumed to be linear elastic. The material parameters that remain constant during the study are shown in **Table 1**.

Table 1: Constant material parameters

Concrete data	
Compressive strength f_{cm} [N/mm^2]	24.73
Tensile strength f_{ctm} [N/mm^2]	1.9
Young's modulus [N/mm^2]	29000
Tensile fracture energy [N/mm]	0.057

Steel data	
Young's modulus [N/mm^2]	200 000

Due to symmetric geometry, only a quarter of the problem's geometry is modelled to optimize the computation time. The geometry is discretized with first-order tetrahedral elements (also referred as SOLID185 elements in ANSYS® documentation [11]). **Figure 1** shows the model geometry and the applied constraints. **Table 2** lists the geometric specifications of the models. The concrete slab consists of two parts which are connected via shared nodes. This division is made in order to apply a finer mesh to concrete inside the support where the breakout takes place. The contact between concrete and headed stud is assumed to be frictionless and is modelled using a penalty based contact formulation. A compression-only support on the bottom of the slab is applied to simulate the effect of a strong floor on which the slab is placed in an experiment.

2.2 Drucker-Prager concrete model

As previously mentioned, a Drucker-Prager concrete model [12] with Rankine's yield surface in tension is employed to model the material response of concrete. The strain softening function under compression can be defined in several ways for this model. Here, the focus is laid on the exponential formulation and the fracture energy-based formulation. It should be noted that for exponential formulation of softening under compression

only tension fracture energy is regularized and for fracture energy-based formulation both tension and compression fracture energies are regularized. The strain softening functions under compression are illustrated in **Figure 2**.

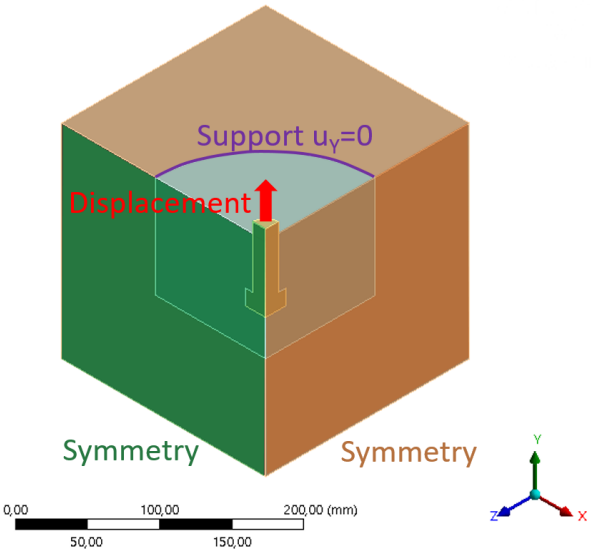

Figure 1: Geometry and constraints of the model

Table 2: Geometric data of the models

Embedment depth	**50 mm**	**70 mm**
Shaft diameter	25 mm	
Head diameter	40 mm	
Head thickness	12 mm	
Full slab dimensions	400 by 400 by 200 mm	720 by 720 by 280 mm
Size inner concrete body	150 (radius) by 100 mm	210 (radius) by 140 mm
Support distance	150 mm	210 mm

In both formulations, the hardening function $\Omega_c\ (\kappa)$ is defined by the following function in the sector $\kappa < \kappa_{cm}$:

$$\Omega_c = \Omega_{ci} + (1 - \Omega_{ci}) \sqrt{2\frac{\kappa}{\kappa_{cm}} - \frac{\kappa^2}{\kappa_{cm}^2}} \qquad (1)$$

In this formula, Ω_{ci} is the relative stress i.e., stress fraction relative to the strength (in other terms the stresses on the y-axis in **Figure 2** are normalized with respect to corresponding strength) at start of nonlinear hardening and κ_{cm} is the plastic strain at uniaxial compressive strength f_c.

The two formulations differ in the definition of the softening function after the uniaxial compressive strength is reached at $\Omega_c = 1$ and $\kappa = \kappa_{cm}$. In the exponential formulation, the softening function in (plastic strain) range $\kappa_{cm} < \kappa < \kappa_{cu}$ is defined by:

$$\Omega_c = 1 - (1 - \Omega_{cu}) \left(\frac{\kappa - \kappa_{cm}}{\kappa_{cu} - \kappa_{cm}} \right)^2 \qquad (2)$$

Here, κ_{cu} is the plastic strain at transition from power law to exponential softening and Ω_{cu} is the respective relative stress (relative to strength) at this point of transition. For $\kappa > \kappa_{cu}$, an exponential softening function follows that converges towards the residual compressive relative stress Ω_{cr} for increasing plastic strain (κ):

$$\Omega_{cu} = \Omega_{cr} \cdot (\Omega_{cu} - \Omega_{cr}) e^{\left(2\frac{\Omega_{cu}-1}{\kappa_{cu}-\kappa_{cm}} \cdot \frac{\kappa-\kappa_{cu}}{\Omega_{cu}-\Omega_{cr}}\right)} \qquad (3)$$

In this exponential softening function, the transition from power law to exponential softening is the governing input parameter for the softening behavior of the material. This transition is defined by the value of Ω_{cu}.

The softening function for the fracture energy-based formulation is defined by a single function for $\kappa > \kappa_{cm}$:

$$\Omega_c = \frac{1}{\alpha_c(\kappa^2 - 2 \cdot \kappa_{cm} \cdot \kappa + \kappa_{cm}^2) + 1}$$

$$\alpha_c = \left(\frac{\pi}{2} \cdot \frac{f_c}{g_{fc}} \right)^2$$

$$g_{fc} = max\left(\frac{G_{fc}}{L_i}, \frac{f_c^2}{E} \right) \qquad (4)$$

There, G_{fc} is the mode I fracture energy in compression, L_i is the effective element length and E is the Young's Modulus.

By this definition, the following relationship between fracture energy and softening function is fulfilled:

$$\int_{\kappa_{cm}}^{\infty} \Omega_c \, d\kappa = \frac{g_{fc}}{f_c} \qquad (5)$$

For this formulation, the governing input parameter for the softening function is the mode I fracture energy in compression G_{fc}.

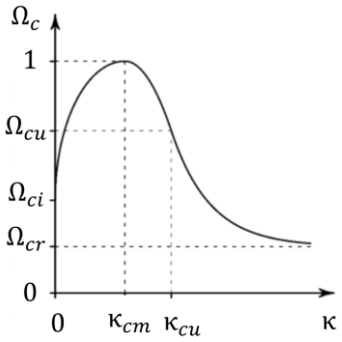

a) Exponential softening

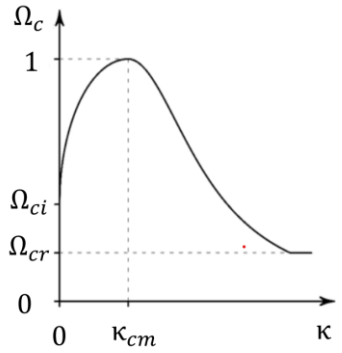

b) Fracture energy-based

Figure 2: Hardening and softening functions under compression [12]

2.3 Investigated fracture energy parameters and mesh sizes

For the study, several variations of fracture energy input parameters were investigated. For the exponential formulation of the softening function, a set of input parameters based on $\Omega_{cu} = 0{,}8$ (model name: E80) was used. Furthermore, a parameter set based on $\Omega_{cu} = 0{,}56$ (E56) was used as this value corresponds to the nominal ultimate strain $\varepsilon_{cu} = 0{,}0035$ which is used in EN 1992-1-1:2011-01[10].

For the fracture energy-based softening formulation, three different sets of material parameters were investigated. The first one (G9,75) was designed in order to replicate the same fracture energy as for the exponential softening curve with $\Omega_{cu} = 0{,}8$ (model name: E80). The compressive fracture energy for the exponential softening is computed using the definition suggested by *Nakamura & Higai* [13] (see **Figure 3**). For the model with exponential softening, the compressive to tensile fracture energy ratio (G_{fc}/G_{ft}) is calculated as 9.75 when the tensile fracture energy is defined according to *Model Code 1990* [14]. This definition of the tensile fracture energy is used for all material parameter sets in this investigation. Comparing this ratio of compressive to tensile fracture energy with experimental values from literature [13,15–17], it can be seen that the computed ratio is much lower than the experimental values of G_{fc}/G_{ft}which are usually in a range of 100 to 150. Thus, two additional sets of concrete input parameters with $G_{fc}/G_{ft} = 50$ (G50) and $G_{fc}/G_{ft} = 100$ (G100) are added to the simulation matrix.

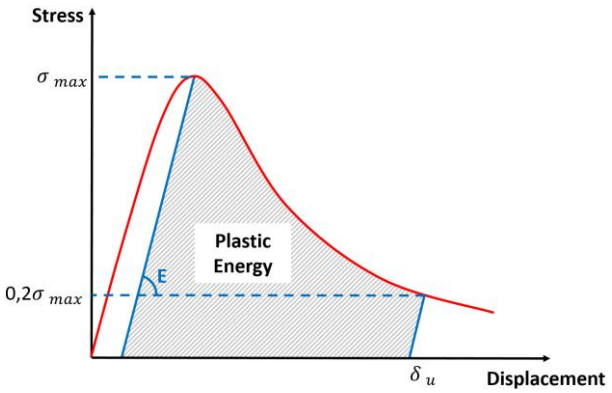

Figure 3: Compressive fracture energy by the definition of Nakamura & Higai [13]

All the simulations were carried out with an average mesh size of 4-5 mm in the inner concrete body in contact with the stud where the CC breakout is expected. In order to investigate the influence of the mesh size, the G9,75 simulations were also carried out with average mesh sizes of ≈ 6 mm (G9,75M6) and ≈ 8 mm (G9,75M8).

3 DISCUSSION OF RESULTS

The simulation results can be evaluated with regard to several aspects. For the simulations with the fracture energy-based softening function, the dependence of the ultimate load on the fracture energy in compression can be seen in **Figure 4** a) for the headed stud with h_{ef} = 50 mm and in **Figure 5** a) for embedment depth h_{ef} = 70 mm. An increase in compressive

fracture energy leads to an increase in predicted peak load but the development is not linear. It is also visible in the load-displacement curves in **Figure 4** c) and **Figure 5** c) that the increase in compressive fracture energy also leads to higher displacement at peak load. The load displacement curves of the G9,75, E80 and E56 simulations are very similar which can barely be distinguishable in the plot. This similarity makes sense given the similarity in the compression fracture energy in the models. The steep drop in the softening branch for G50 and G100 with h_{ef} = 50 mm comes from a splitting crack opening in the concrete slab.

When looking at the results of the mesh sensitivity study in **Figure 4** b) and **Figure 5** b), it is visible that the regularization process works fairly well as the ultimate loads vary very little. Still, a slight change of ultimate loads with increasing mesh size can be recognized. Interestingly, the ultimate load tends to decrease with growing mesh size for embedment depth h_{ef} = 50 mm but for h_{ef} = 70 mm it tends to increase.

In **Figure 6**, the fracture pattern at peak load are shown for the G9,75 and G100 simulation with h_{ef} = 50 mm. It is visible that the fracture at peak load is more pronounced in the model with the higher fracture energy. Given the fact that the displacement at peak load is much higher in this simulation this is expectable. While the initial cracking looks similar for both fracture energies, the shape of the concrete cone differs. The models with lower fracture energy have a steeper fracture angle and thus a smaller-sized concrete cone as it is shown in **Figure 7**.

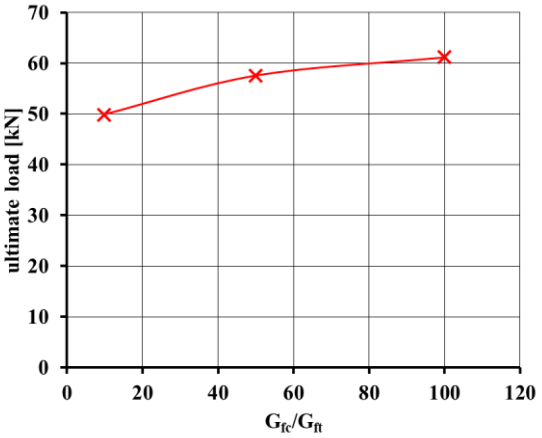

a) Ultimate load over fracture energy

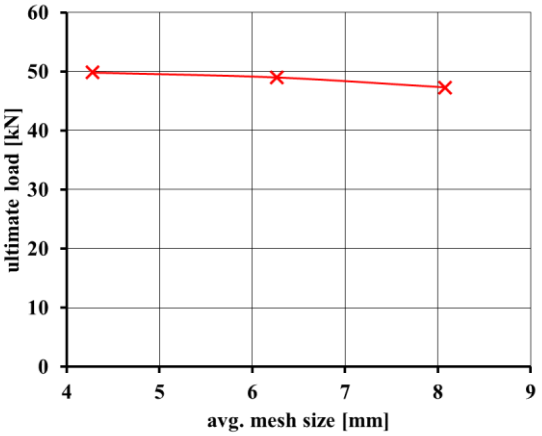

b) Ultimate load over average mesh size

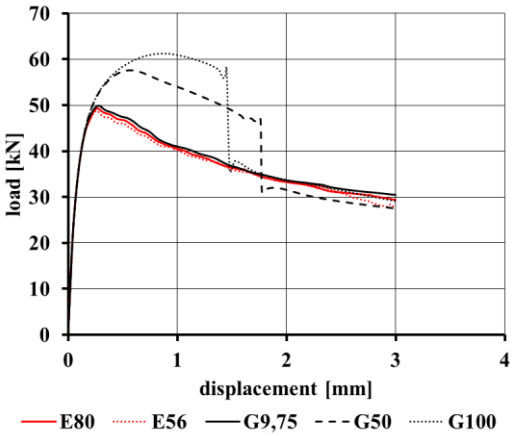

c) Load-displacement curves

Figure 4: Simulation results of the simulations with h_{ef} = 50 mm

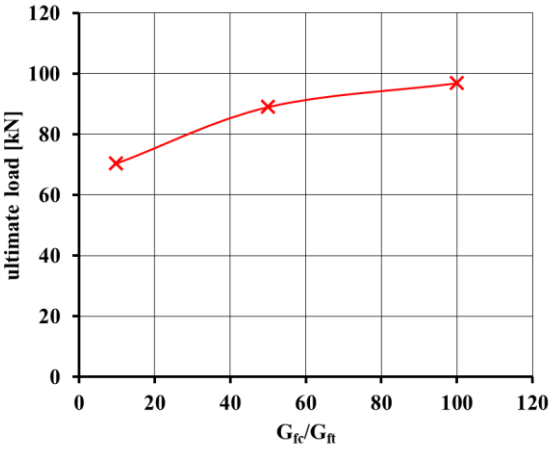

a) Ultimate load over fracture energy

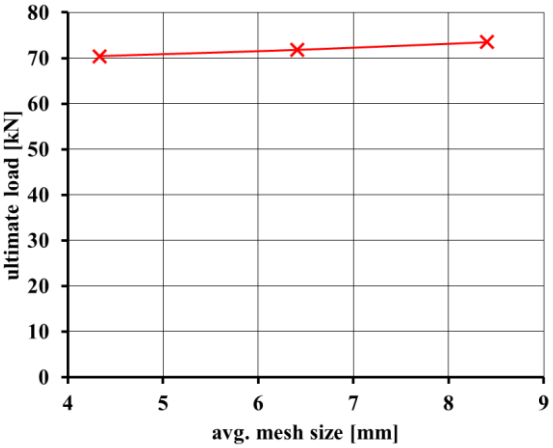

b) Ultimate load over average mesh size

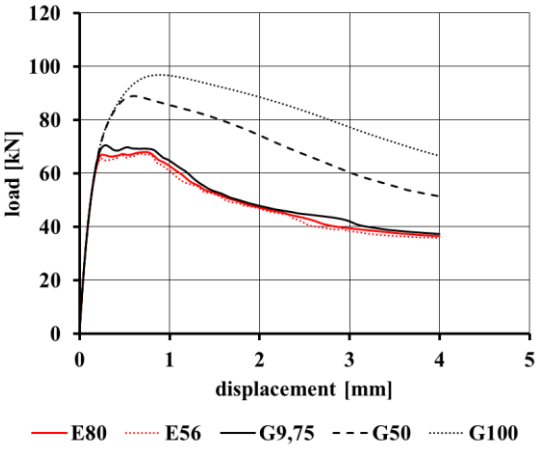

c) Load-displacement curves

Figure 5: Simulation results of the simulations with h_{ef} = 70 mm

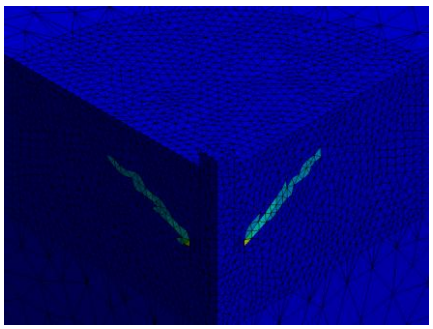

a) G9,75 material data

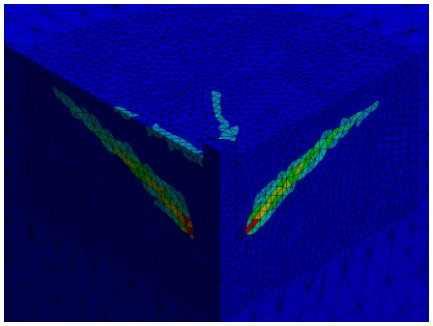

b) G100 material data

Figure 6: Fracture pattern at peak load for embedment depth h_{ef} = 50 mm

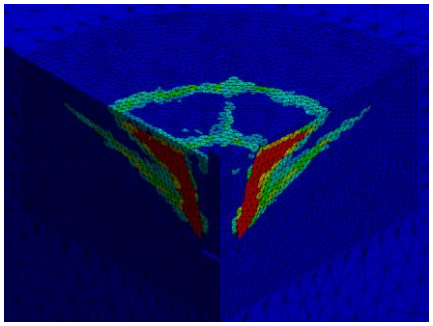

a) G9,75 material data

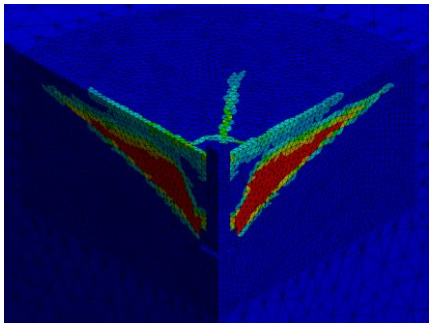

b) G100 material data

Figure 7: Fracture pattern at 4 mm displacement for embedment depth h_{ef} = 70 mm

It is interesting to see that the Drucker-Prager model with the exponential softening ends up with a very low ratio of compressive fracture energy to tensile fracture energy. This ratio of G_{fc}/G_{ft} is only around 10% which is very less as compared to the values which can be found in literature [13,15–17]. This discrepancy also leads to significant changes in ultimate load, load-displacement behavior and fracture pattern.

4 CONCLUSIONS

In the presented paper, the influence of the fracture energy under compression was investigated in a numerical study. A Drucker-Prager concrete model with Rankine's surface i.e., the yield surface under compression is defined using Drucker-Prager criterion and the Rankine criterion bounds the tensile stresses for concrete, was used with two different formulations of the softening function viz., exponential (without regularization of compression fracture energy) and fracture energy-based softening (with regularization of both compression and tension fracture energy). It could be seen in simulation that an increase in compressive fracture energy leads to a higher peak load and a change in load-displacement behavior. Furthermore, the fracture angle of the concrete cone and thus the size of it was found to be significantly influenced by the compressive fracture energy. For the mesh-sensitivity of the model, slight changes of ultimate load over mesh size but no clear tendency could be seen.

In the ratio of compressive to tension fracture energy, there are large differences between the material input parameters used with the exponential softening function and the ones with fracture energies according to experimental results from literature. This difference of roughly factor 10 contributes to the differences in ultimate load and load-displacement behavior.

It is up to further investigations to validate the approach of defining the material softening parameters of concrete to correctly simulate the complex fracture processes of CC-failure more realistically.

REFERENCES

[1] Holder, J., Lakhani, H. and Hofmann, J., 2024. Influence of Different Modelling Approaches on the Predicted Concrete Edge Failure of Fasteners. *fib Symposium Christchurch*.

[2] Lakhani, H., Holder, J. and Hofmann, J., 2024. Effect of Bond on the Shear Capacity of Reinforced Concrete Beams: Comparison of Different FE Models. *fib Symposium Christchurch*.

[3] Holder, J., Lakhani, H. and Hofmann, J., 2024. Use of Numerical Simulations for the Design of Fasteners – Limitations and Way Forward. *fib PhD Symposium Budapest*.

[4] Bažant, Z. and Oh, B. H., 1983. Crack Band Theory for Fracture of Concrete. *Mater. Struct.* **16**:155–177.

[5] Jirásek, M., and Bauer, M., 2012. Numerical Aspects of the Crack Band Approach. *Comput. Struct.* **110–111**:60–78.

[6] Červenka, J., Červenka, V. and Laserna, S., 2018. On Crack Band Model in Finite Element Analysis of Concrete Fracture in Engineering Practice. *Eng. Fract. Mech.* **197**:27–47.

[7] Eligehausen, R. and Sawade, G., 1989. A Fracture Mechanics Based Description of the Pull-out Behavior of Headed Studs Embedded in Concrete. In Elfgren, L. (ed), *Fracture Mechanics of Concrete Structures;* pp.281–299.

[8] Ozbolt, J., 1995. *Maßstabseffekt und Duktilität von Beton und Stahlbetonkonstruktionen*. Habilitation in German, University of Stuttgart.

[9] ANSYS Inc., 2023. *ANSYS® Academic Research Mechanical*. Release 2023 R2.

[10] DIN, 2011. *EN 1992-1-1 Eurocode 2: Design of Concrete Structures – Part 1-1: General Rules and Rules for Buildings*.

[11] ANSYS Inc., 2023. *ANSYS Help Mechanical APDL 2023 R2*, Help System. Element Reference Chapter 7. SOLID185.

[12] ANSYS Inc., 2023. *ANSYS Help Mechanical APDL 2023 R2*, Help System. Material Reference Chapter 4.11 Geomechanics.

[13] Nakamura, H. and Higai, T., 2001. Compressive Fracture Energy and Fracture Zone Length of Concrete. In Shing P. B., Tanabe T.-A. (eds), *Modeling of Inelastic Behavior of RC Structures under Seismic Loads;* pp.471–487.

[14] CEB-FIP, 1993. *Model Code 1990: Design Code*. T. Telford Ltd.

[15] Nakamura, H., Nanri, T., Miura, T. and Sushanta, R., 2018. Experimental Investigation of Compressive Strength and Compressive Fracture Energy of Longitudinally Cracked Concrete. *Cem. Concr. Compos.* **93**:1–18.

[16] Lertsrisakulrat, T., Watanabe, K., Matsuo, M. and Niwa, J., 2001. Experimental Study on Parameters in Localization of Concrete Subjected to Compression. *Mater. Concr. Struct. Pavements JSCE* **669(V50)**:309–321.

[17] Rokugo, K. and Koyanagi, W., 1992. Role of Compressive Fracture Energy of Concrete on the Failure Behavior of Reinforced Concrete Beams. In Carpinteri A. (ed), *Applications of Fracture Mechanics to Reinforced Concrete;* pp. 437–464.